Violation of a Leggett–Garg inequality using ideal negative measurements in neutron interferometry

Elisabeth Kreuzgruber[1],* Richard Wagner[1], Niels Geerits[1], Hartmut Lemmel[1,2], and Stephan Sponar[1†]

[1]*Atominstitut, TU Wien, Stadionallee 2, 1020 Vienna, Austria*
[2]*Institut Laue-Langevin, 38000, Grenoble, France*
(Dated: October 24, 2023)

We report on an experiment that demonstrates the violation of a Leggett–Garg inequality (LGI) with neutrons. LGIs have been proposed in order to assess how far the predictions of quantum mechanics defy 'macroscopic realism'. With LGIs, correlations of measurements performed on a single system at different times are described. The measured value of $K = 1.120 \pm 0.007$, obtained in a neutron interferometric experiment, is clearly above the limit $K = 1$ predicted by macro-realistic theories.

Introduction.—The question whether measurable quantities of a quantum object have definite values prior to the actual measurement is a fundamental issue ever since quantum theory has been introduced more than a century ago. Examples include Bell's inequality [1, 2], which sets bounds on correlations between measurement results of space-like separated components of a composite (entangled) system. A violation of Bell's inequality thus demonstrates that certain predictions of quantum mechanics cannot be reproduced by realistic theories, more precisely, by local hidden variable theories (LHVT). Another prime example is found in the Kochen–Specker theorem [3], which stresses the incompatibility of quantum mechanics with a larger class of hidden-variable theories, known as noncontextual hidden-variable theories (NCHVTs). Here it is assumed that the result of a measurement of an observable is predetermined and independent of a suitable (previous or simultaneous) measurement of any other compatible (co-measurable or commuting) observable, i.e., the measurement context. While both Bell's inequality and tests of the Kochen–Specker theorem require composite or multiple spatially-separated systems, Leggett–Garg inequalities (LGIs) [4] study temporal correlations of a single system; therefore they are often referred to as Bell inequalities *in time.*

Violation of a Bell inequality is a direct witness of entanglement - a very specific feature of quantum mechanics. Contrary, in the case of LGIs, the violation occurs due to the *coherent superposition* of system states, which is essentially the most fundamental property of quantum mechanics. In other words, LGIs quantify coherence in quantum systems and can consequently be seen as a measure or test of *quantumness.*

Leggett–Garg inequalities were proposed in 1985 [4] in order to assess whether sets of pairs of sequential measurements on a single quantum system can be consistent with an underlying macro-realistic theory [5]. Within the framework of a macro-realistic theory, a single macroscopic system fulfills the following two assumptions of macrorealism measured at successive times: (A1) at any given time the system is always in only one of its macroscopically distinguishable states, and (A2) the state of the system can be determined in a non-invasive way, meaning without disturbing the subsequent dynamics of the system. Quantum mechanics predicts the violation of the inequalities since it contradicts both assumptions (A1) and (A2). The (quantum) system under observation has to be measured at different times. Correlations that can be derived from sequences of this measurements let us formulate the LGI. The results of these correlation measurements either confirm the absence of a realistic description of the system or the impossibility of measuring the system without disturbing it [5]. This will also refuse a well-defined pre-existing value of a measurement. Recent violations of LGIs have been observed in various systems, including photonic qubits [6–9], nuclear spins in a diamond defect center[10], superconducting qubits in terms of transoms [11] and flux qubits [12], nuclear magnetic resonance [13, 14], and spin-bearing phosphorus impurities in silicon [15]. Proposed schemes for increasing violations of Leggett–Garg inequalities range from action of an environment on a single qubit in terms of generic quantum channels [16] to open many-body systems in the presence of a nonequilibrium [17]. In a recent paper [18] the authors propose to test a violation of the Leggett–Garg inequality due to the gravitational interaction in a hybrid system consisting of a harmonic oscillator and a spatially localized superposed particle [19], aiming to probe the *quantumness* of gravity [20, 21].

The violation of an LGI in an interferometric setup has been proposed in literature theoretically for electrons in [22]. The requirement of non-invasive measurements from (A2) is realized in most experiments by utilizing the concept of weak measurements, or by introducing an ancilla system, as implemented in [15]. Note that even a weak measurement can in practice never be completely non-invasive (due to a non-vanishing measurement strength) and the preparation of the ancilla system will also always be imperfect. However, the experimental procedure from [22] realizes *ideal negative measurements* in an interferometer experiment in order to fulfill the requirement of non-invasive measurements from (A2) without the need for an ancilla. An ideal

negative measurement is an interaction-free measurement that avoids any direct interaction with the system under investigation, since it probes the *absence* rather than the *presence* of an object [22].

In this Letter, we present a neutron interferometric experiment, demonstrating a violation of the LGI. In our measurement scheme the single system is represented by the neutron's path in an interferometer. Criteria for quantifying the degree of macroscopicity of superposition states have long been discussed [23, 24], resulting in a general agreement that the macroscopicity increases either with heavier masses or larger spatial separations of the superposition states. The macroscopic beam separation, accounting for the macroscopicity of superposition state, of several centimeters makes neutron interferometry therefore particularly suited to test LGIs.

Leggett–Garg inequality.—For dichotomous variables Q_i, accounting for two *macroscopically distinguishable* states having outcomes $q_i = \pm 1$, the correlation function for measurements at times t_i, t_j is given by

$$C_{ij} = \langle Q_i Q_j \rangle = \sum_{q_i q_j = \pm} q_i q_j P\big(q_i(t_i), q_j(t_j)\big), \quad (1)$$

where $P(q_i(t_i), q_j(t_j))$ denotes the *joint* probability of obtaining the measurement results q_i at time t_i and q_j at time t_j. Considering Eq.(1) for three experimental sets with $i, j \in \{1, 2, 3\}$ yields ~~the LGI~~

$$K \equiv C_{21} + C_{32} - C_{31}, \quad (2)$$

where K denotes the *Leggett–Garg correlator*, with limits $-3 \leq K \leq 1$; that is the LGI. Since the three correlators are derived from probabilities with $|C_{ij}| \leq 1$, the lower limit cannot be violated. However, quantum mechanics allows for a violation of the upper bound. In a two-level system, the maximum obtainable violation is $K = 1.5$ [5].

The basic idea behind the experimental procedure, as proposed by Emary et al. in [22], is to map the temporal structure (or measurement time t_i) of the LGI onto real-space coordinates, more precisely onto three distinct regions of the interferometer, indicated by the index $\alpha \in \{1, 2, 3\}$, cf. Fig. 1. Within each region, the two paths of the interferometer constitute a qubit. The measurement of the qubit's state, denoted as $q_i = \pm 1$, therefore results in a "which-way" measurement [25] in the particular region of interest. While a click of a detector in e.g. the + arm of region 2 ($q_2 = +1$) is a strongly *invasive measurement*, on the other hand the absence of a detector response implies $q_2 = -1$ without any direct interaction. ~~does not disturb the system at all~~. It accounts for the required non-invasive measurement (A2) in terms of an *ideal negative measurement*.

In our neutron interferometric realization of [22], neutrons enter the interferometer via the + port of region 1. Hence, the initial state is known and therefore it is
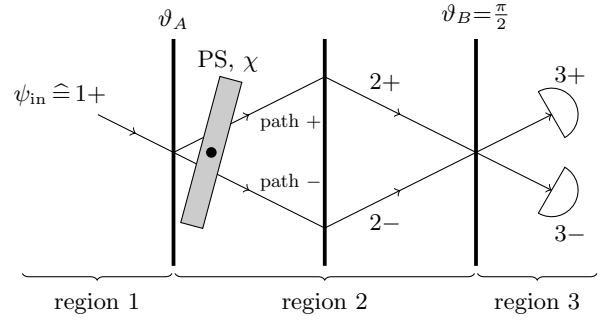

FIG. 1: Regions in the Mach-Zehnder interferometer and setup for determination of correlator C_{31}.

not necessary to measure in region 1. ~~the noninvasive measurability is granted~~. The first plate of the interferometer consists of a tunable beamsplitter characterized by parameter ϑ_A, which is schematically illustrated in Fig. 1. The theoretical maximum of $K = 1.5$ is obtained for $\vartheta_A = \vartheta_B = \pi/3$ and phase shift $\chi = 0$. However, in our setup we fixed $\vartheta_B = \pi/2$ (usual 50:50 beamsplitter), since a non 50:50 beamsplitter requires additional absorbers, which is explained in detail in the experimental Section. Then, the maximal possible violation is $K = \sqrt{2}$, for $\vartheta_A = \pi/4$.

We define $P_{\alpha\pm,\beta\pm}(n_\alpha, n_\beta)$ as the joint probability that two detectors placed at position $\alpha\pm$ and $\beta\pm$ respectively detect ($n = 1$) or don't detect a neutron ($n = 0$), where α and β specify the region and $\pm$ the path. Then the correlator, as defined in Eq.(1), between regions α and β is given by

$$C_{\alpha\beta} = \sum_{q_\alpha, q_\beta = \pm} q_\alpha q_\beta P_{\alpha q_\alpha, \beta q_\beta}(1, 1). \quad (3)$$
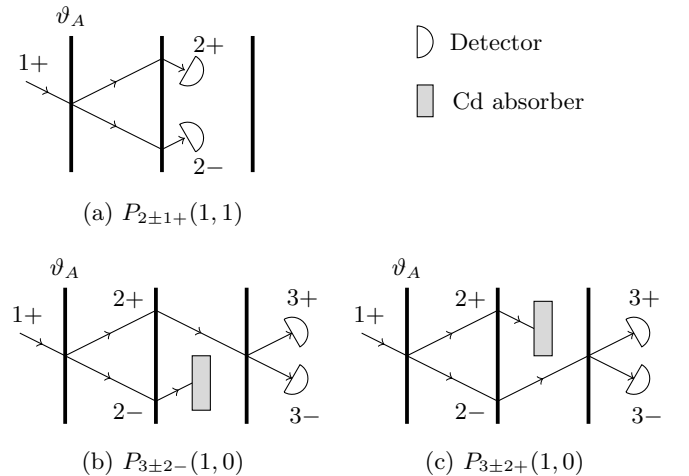
Hence the correlation function for regions 1 and 3,

(a) $P_{2\pm 1+}(1, 1)$

(b) $P_{3\pm 2-}(1, 0)$ (c) $P_{3\pm 2+}(1, 0)$

FIG. 2: Setups to determine probabilities $P_{2\pm 1+}$ for correlators C_{21} in (a) and $P_{3\pm 2\pm}$ for C_{32} in (b),(c).
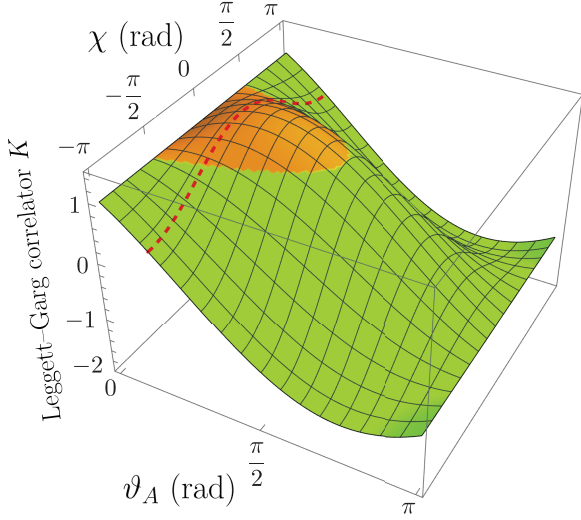
FIG. 3: Regions in the parameter space where the LGI can be violated, with fixed $\vartheta_B = \pi/2$. The dashed red line indicates our experimental parameter settings.

denoted as C_{31}, can simply be expressed as $C_{31} = P_{3+,1+}(1,1) - P_{3-,1+}(1,1)$, since the neutrons always enter from $1+$. Therefore, the correlation function C_{31} can also be expressed in terms of marginal probabilities as $C_{31} = P_{3+}(1) - P_{3-}(1)$. Although not particularly necessary here, it is instructive to express C_{31} in terms of *ideal negative* measurements as

$$C_{31} = \sum_{q_1,q_3=\pm} q_1 q_3 P_{3q_\alpha}(1)\left(1 - P_{1q_\beta}(0)\right)$$
$$= -\sum_{q_1,q_3=\pm} q_1 q_3 P_{1q_2,3q_3}(1,0), \qquad (4)$$

since $P_{1q_1}(0) = 1 - P_{1q_1}(1)$. A similar expression gives the correlator $C_{21} = P_{1+,2+}(1) - P_{1+,2-}(1)$ which is measured with detectors directly placed in region 2, shown in Fig. 2(a).

For C_{32}, all four terms of the sum from Eq.(3) contribute, taking both paths of section 2 into account.

$$C_{32} = \sum_{q_2,q_3=\pm} q_2 q_3 P_{3q_3,2q_2}(1,1) \qquad (5)$$

Using again $P_{2q_2}(0) = 1 - P_{2q_2}(1)$ we write the sum as

$$C_{32} = -\sum_{q_2,q_3=\pm} q_2 q_3 P_{3q_3,2q_2}(1,0) \qquad (6)$$

in order to account for the non-invasive or ideal negative measurement in section 2. The two probabilities $P_{3\pm,2-}(1,0)$ are determined by counting the neutrons in path $3+$ and $3-$ respectively under the condition that they have not been counted in path $2-$. The latter is ensured by placing a beam blocker in path $2-$, cf.

Fig. 2(b). The other two probabilities are measured similarly as shown in Fig. 2(c).

The correlators according to [22] for the regions in our setup are calculated as follows

$$\begin{aligned} C_{21} &= \cos\vartheta_A \\ C_{32} &= \cos\vartheta_B \\ C_{31} &= \cos\vartheta_A \cos\vartheta_B - \cos\chi \sin\vartheta_A \sin\vartheta_B \qquad (7) \\ K &= \cos\vartheta_A + \cos\vartheta_B - \cos\vartheta_A \cos\vartheta_B \\ &\quad + \cos\chi \sin\vartheta_A \sin\vartheta_B, \end{aligned}$$

which in our setup, with fixed $\sin\vartheta_B = \frac{\pi}{2}$, K becomes

$$K = \cos\vartheta_A + \cos\chi \sin\vartheta_A. \qquad (8)$$

Figure 3 shows the regions in the parameter space (ϑ_A,χ) of our experimental LGI test (with fixed value $\vartheta_B = \pi/2$), where it is in theory possible to violate the LGI with a value $K = \sqrt{2}$. ϑ_A represents the mixing angle of the first interferometer plate, and χ the phase shifter angle. The resulting K values are shown in green for areas where no violation is possible, and in orange for a possible violation of the LGI. The dashed red line indicates our measurement result in an ideal interferometer.

Neutron interferometer setup.—Neutron interferometry [26, 27] provides a powerful tool for investigation of fundamental quantum mechanical phenomena. Entanglement between different degrees of freedom (DOF), e.g., the neutron's spin, path, and energy DOF has been confirmed, and the contextual nature of quantum mechanics has been demonstrated successfully [28]. In more recent experiments, the concept of weak measurements and weak values has been utilized for direct state reconstruction [29], demonstration of the canonical commutator relation [30] and studies of "which-way" information [31, 32].

The experiment was carried out at the neutron interferometer instrument S18 at the high-flux reactor of the Institute Laue-Langevin (ILL) in Grenoble, France (the experimental data can be found on the ILL data server under [33]. A monochromatic unpolarized neutron beam with mean wavelength $\lambda = 1.91$Å ($\delta\lambda/\lambda \sim 0.02$) and $3 \times 3\,\mathrm{mm}^2$ beam cross section was used to illuminate the interferometer. In order to observe a violation of an LGI in an interferometric experiment, it is necessary to implement a non-50:50 beam splitter at the first plate of the interferometer. This is achieved by placing a partial absorber behind the first interferometer plate in one of the neutron paths. The absorber is an Indium slab, about 3 mm thick, placed in path I, resulting in an intensity ratio between paths I and II of about 10:90. The interferometer itself is a symmetric three-plate silicon perfect crystal (triple Laue type), with a plate thickness of 3 mm and a length of 140 mm. A schematic illustration of the interferometric setup is given in Fig. 4. To obtain
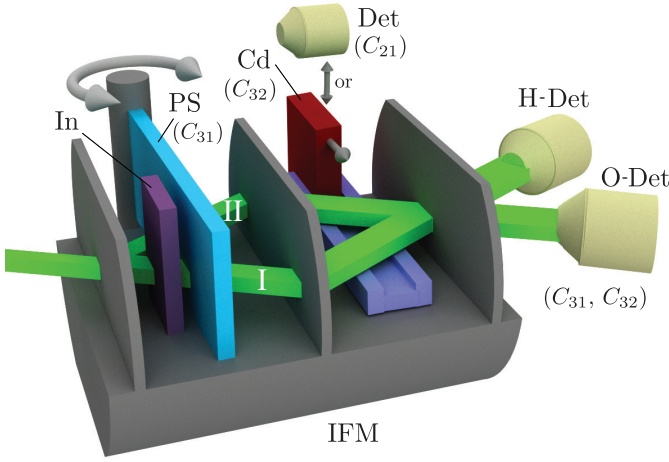
FIG. 4: Unpolarized monochromatic neutrons enter the interferometer and are split into paths I and II. Green indicates the neutron beam, blue the phase shifter and purple the Indium absorber. Detectors O (front) and H (back) as well as the (re)movable detector for C_{21} measurement and Cadmium blocker (red) are shown.

interference fringes, a 5 mm Aluminium phase shifter is used. Additional beam blockers for the detection of single path intensities were made of Cadmium. Both the 'O' and 'H' detectors outside the interferometer and the additional detector for C_{21} measurements were ^{3}He proportional counting tubes.

Determination of correlators C_{31} and C_{21} is straightforward. In both cases it is not necessary to measure non-invasively, since no subsequent measurement on the same state is performed. For C_{31}, the measurement is that of a standard interferogram Fig. 5, with measurement time 180 seconds per phase shifter position. The correlator C_{31} is calculated via

$$C_{31} = \frac{N_{3+1+}(\chi) - N_{3-1+}(\chi)}{N_{3+1+}(\chi) + N_{3-1+}(\chi)}, \qquad (9)$$

where $N_{3+1+}(\chi)$ denotes the counts in the H detector and $N_{3-1+}(\chi)$ the counts in the O detector. Due to the cosine behaviour of the recorded interferogram, this correlator is dependent on the position χ of the phase shifter. For the largest possible violation, the maximum counts in O and minimum in H are used, which corresponds to the position $\chi = 2n\pi$ (where $n \in \mathbb{N}_0$) in Fig. 5.

Similarly, the correlator C_{21} is calculated as

$$C_{21} = \frac{N_{2+1+} - N_{2-1+}}{N_{2+1+} + N_{2-1+}} \qquad (10)$$

and is performed as a transversal scan with a pencil-size ^{3}He detector mounted on a translation stage in region 2 of the interferometer, with measurement time 300 seconds per detector position. Moving first through path I and then through path II, the resulting neutron counts are
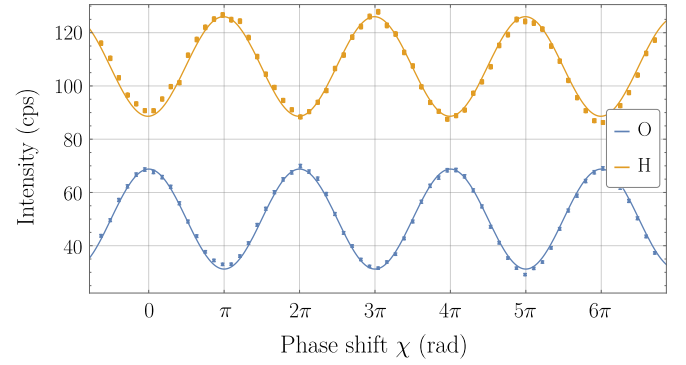

FIG. 5: Measurement results for the of C_{31} correlator in terms of interferograms.

shown in Fig. 6, where the separation between both paths is also clearly visible. Note that only for determination of the correlator C_{21} we make use of a fair sampling assumption, since the detector does not cover the entire beam cross section of path I and II simultaneously. ~~which is the case for a wide range of experiments of this kind, since simultaneous detection of everything is impossible.~~ The N_{2i1+} are the neutron counts in the peak of the respective Gaussian fit to the intensity profiles.

For correlator C_{32} however, it is crucial to measure non-invasively. This is done by measuring the *absence* of a neutron in a given path due to the Cd blocker, meaning that the neutron has to take the path without the Cd blocker. This is represented by the minus sign in Eq. (6). Four measurements are performed, with each of the paths blocked in turn and the resulting intensity in detectors O and H recorded for a measurement time of 600 seconds. These results are shown in Fig. 7. C_{32} becomes

$$C_{32} = \frac{N_{3+2-} + N_{3-2+} - N_{3+2+} - N_{3-2-}}{N_{3+2-} + N_{3-2+} + N_{3+2+} + N_{3-2-}}, \qquad (11)$$

with N_{3+2-} and N_{3+2+} the neutron counts in the H detector with blocked path II and path I, respectively, and likewise for the O detector in $N_{3-2\pm}$.
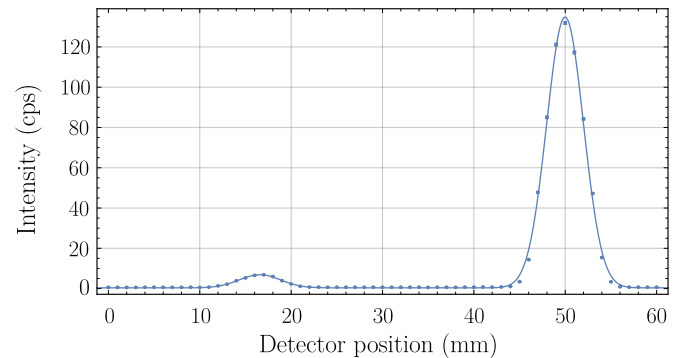

FIG. 6: Measurement results for the of C_{21} correlator obtained by a transversal scan of movable detector.
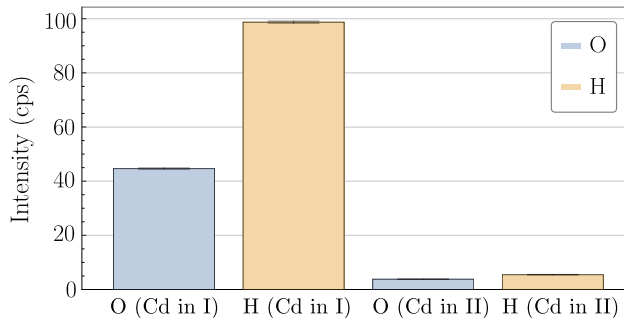
FIG. 7: Measurement results for the of C_{32} correlator: neutron counts in detectors O (blue) and H (orange).

Results.—In order to demonstrate the experimental violation of the Leggett–Garg inequality, we calculate the correlator K, Eq. (2). The resulting curve is shown in Fig. 8, with the maximum at a phase shift of $\chi = 0$. With the Indium absorber in path I of the interferometer, a violation of the limit $K = 1$ is clearly visible (Fig. 8(a)). Our results show a significant violation of the LGI by 18 standard deviations σ (denoted as $n_\sigma = 18$) at the maximum, $K = 1.120 \pm 0.007$. The violation is visible over a wide range of phase shifter values χ. Numeric values of the individual correlators C_{ij} and the final value of K in case of the maximal violation of the LGI are presented in Tab. I. For comparison, Fig. 8(b) shows the same measurement procedure for a symmetric beam splitter ($\vartheta_A = \pi/2$), i.e. without absorber, where no violation is possible, resulting in $K = 0.540 \pm 0.023$. The main reason for the deviation of our final result $K = 1.120 \pm 0.007$ from the theoretically predicted value $K = \sqrt{2}$ is the fact that our 3 mm Indium absorber, used for the asymmetric beam splitter, corresponds to $\vartheta_A \sim 0.15\,\pi$ rather than $\vartheta_A = \pi/4$. This reduces the maximal obtainable K value from $K = \sqrt{2}$ to $K \sim 1.34$. Furthermore, correlator C_{31} strongly depends on the fringe contrast of the underlying interferograms. The observed contrasts of $C_O = 0.37 \pm 0.008$ and $C_H = 0.17 \pm 0.003$, for O and H beam respectively, are lower than the theoretical prediction of $C_O^\star = 0.45$ and $C_H^\star = 0.21$. If this is taken into account the value of C_{31} is halved.

TABLE I: Results of the three correlators C_{ij} and the Leggett–Garg parameter K for violation of the LGI.

C_{21}	C_{32}	C_{31}	K
0.903 ± 0.002	0.343 ± 0.002	0.126 ± 0.006	1.120 ± 0.007

Concluding remarks and discussion.—Our measurement results demonstrate a violation of an LGI by $n_\sigma = 18.0$, while the absorberless measurements show no violation. Hence, we conclude ~~that neutrons in an interferometer must be understood quantum mechanically.~~ that the obtained results cannot be explained within the framework of macrorealistic theories and are clearly in favour of the
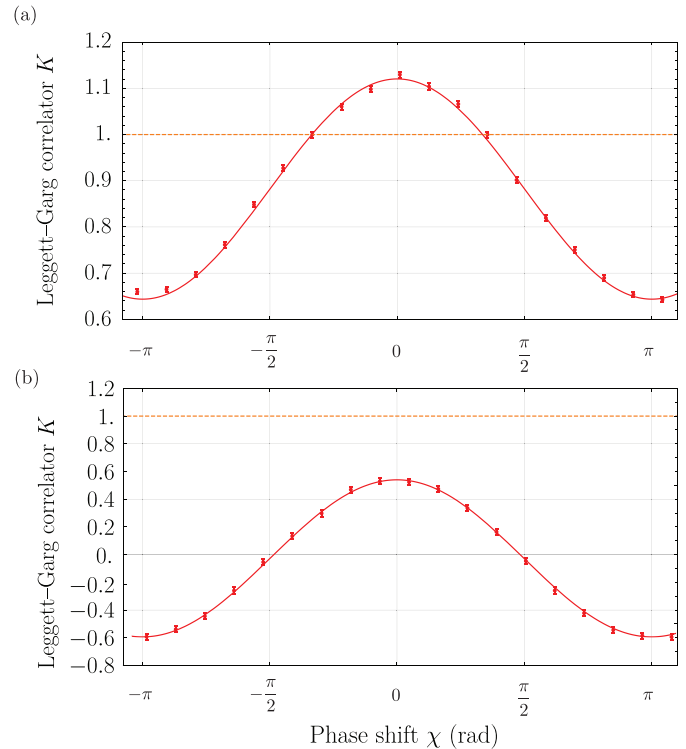

FIG. 8: Results of the violation measurements. The dashed line indicates the limit of $K = 1$. (a) With Indium absorber a maximal violation is observed at $\chi = 0$ and (b) without absorber no violation occurs.

prediction of quantum mechanics.

An even higher violation can be achieved when the signs in region 3 are switched, and detector O becomes 3+, detector H 3−. The correlators C_{31} and C_{32} have to be recalculated accordingly, resulting in $K = 1.162 \pm 0.006$ with $n_\sigma = 28$. This 'additional' violation is due to the asymmetric nature of the perfect crystal interferometer. Since successive reflections on the crystal lamellas enhance the reflectivity [34] the H detector always receives some phase-independent intensity offset. The detection loophole is closed due to the high efficiency of our neutron detectors, close to unity.

At this point we want to briefly discuss weather an ideal negative measurement has a potential impact on our perception of the system in general. Due to the non-invasive character of an ideal negative measurement there is no real change of the system. Nevertheless it affects the description of the system because our knowledge changes due to the measurement outcome, but this does not undermine the conclusions drawn from the violation of the LGI.

Finally, we want to emphasize that the interferometric scheme applied in the present work is not limited to neutrons, but is in fact completely general and can be used for any quantum particle with nonzero or even zero mass.

————————

* ekreuzgruber@gmail.com

† stephan.sponar@tuwien.ac.at

[1] J. S. Bell, On the Einstein-Podolsky-Rosen paradox, Physics (Long Island City, N.Y.) **1**, 195 (1964).

[2] J. S. Bell, On the problem of hidden variables in quantum mechanics, Rev. Mod. Phys. **38**, 447 (1966).

[3] S. Kochen and E. P. Specker, The problem of hidden variables in quantum mechanics, J. Math. Mech. **17**, 59 (1967).

[4] A. J. Leggett and A. Garg, Quantum mechanics versus macroscopic realism: Is the flux there when nobody looks?, Phys. Rev. Lett. **54**, 857 (1985).

[5] C. Emary, N. Lambert, and F. Nori, Leggett–Garg inequalities, Rep. Prog. Phys. **77**, 016001 (2014).

[6] R. Ruskov, A. N. Korotkov, and A. Mizel, Signatures of quantum behavior in single-qubit weak measurements, Phys. Rev. Lett. **96**, 200404 (2006).

[7] A. N. Jordan, A. N. Korotkov, and M. Büttiker, Leggett-garg inequality with a kicked quantum pump, Phys. Rev. Lett. **97**, 026805 (2006).

[8] J. Dressel, C. J. Broadbent, J. C. Howell, and A. N. Jordan, Experimental violation of two-party Leggett-Garg inequalities with semiweak measurements, Phys. Rev. Lett. **106**, 040402 (2011).

[9] M. E. Goggin, M. P. Almeida, M. Barbieri, B. P. Lanyon, J. L. O'Brien, A. G. White, and G. J. Pryde, Violation of the Leggett–Garg inequality with weak measurements of photons, Proc. Natl. Acad. Sci. USA **108**, 1256 (2011).

[10] G. Waldherr, P. Neumann, S. F. Huelga, F. Jelezko, and J. Wrachtrup, Violation of a temporal Bell inequality for single spins in a diamond defect center, Phys. Rev. Lett. **107**, 090401 (2011).

[11] A. Palacios-Laloy, F. Mallet, F. Nguyen, P. Bertet, D. Vion, D. Esteve, and A. N. Korotkov, Experimental violation of a bell's inequality in time with weak measurement, Nat. Phys. **6**, 442 (2010).

[12] G. C. Knee, K. Kakuyanagi, M.-C. Yeh, Y. Matsuzaki, H. Toida, H. Yamaguchi, S. Saito, A. J. Leggett, and W. J. Munro, A strict experimental test of macroscopic realism in a superconducting flux qubit, Nat. Commun. **7**, 13253 (2016).

[13] V. Athalye, S. S. Roy, and T. S. Mahesh, Investigation of the Leggett-Garg inequality for precessing nuclear spins, Phys. Rev. Lett. **107**, 130402 (2011).

[14] A. M. Souza, I. S. Oliveira, and R. S. Sarthour, A scattering quantum circuit for measuring Bell's time inequality: a nuclear magnetic resonance demonstration using maximally mixed states, New J. Phys. **13**, 053023 (2011).

[15] G. C. Knee, S. Simmons, E. M. Gauger, J. J. Morton, H. Riemann, N. V. Abrosimov, P. Becker, H.-J. Pohl, K. M. Itoh, M. L. Thewalt, G. A. D. Briggs, and S. C. Benjamin, Violation of a Leggett–Garg inequality with ideal non-invasive measurements, Nat. Commun. **3**, 606 (2012).

[16] C. Emary, Decoherence and maximal violations of the Leggett-Garg inequality, Phys. Rev. A **87**, 032106 (2013).

[17] J. J. Mendoza-Arenas, F. J. Gómez-Ruiz, F. J. Rodríguez, and L. Quiroga, Enhancing violations of Leggett-Garg inequalities in nonequilibrium correlated many-body systems by interactions and decoherence, Sci. Rep. **9**, 17772 (2019).

[18] A. Matsumura, Y. Nambu, and K. Yamamoto, Leggett-Garg inequalities for testing quantumness of gravity, Phys. Rev. A **106**, 012214 (2022).

[19] S. Bose, D. Home, and S. Mal, Nonclassicality of the harmonic-oscillator coherent state persisting up to the macroscopic domain, Phys. Rev. Lett. **120**, 210402 (2018).

[20] S. Bose, A. Mazumdar, G. W. Morley, H. Ulbricht, M. Toroš, M. Paternostro, A. A. Geraci, P. F. Barker, M. S. Kim, and G. Milburn, Spin entanglement witness for quantum gravity, Phys. Rev. Lett. **119**, 240401 (2017).

[21] C. Marletto and V. Vedral, Gravitationally induced entanglement between two massive particles is sufficient evidence of quantum effects in gravity, Phys. Rev. Lett. **119**, 240402 (2017).

[22] C. Emary, N. Lambert, and F. Nori, Leggett-Garg inequality in electron interferometers, **86**, Phys. Rev. B **86** (2012).

[23] S. Nimmrichter and K. Hornberger, Macroscopicity of mechanical quantum superposition states, Phys. Rev. Lett. **110**, 160403 (2013).

[24] C. Robens, W. Alt, D. Meschede, C. Emary, and A. Alberti, Ideal negative measurements in quantum walks disprove theories based on classical trajectories, Phys. Rev. X **5**, 011003 (2015) .

[25] B.-G. Englert, Fringe visibility and which-way information: An inequality, Phys. Rev. Lett. **77**, 2154 (1996).

[26] H. Rauch and S. A. Werner, *Neutron Interferometry* (Clarendon Press, Oxford, 2000).

[27] J. Klepp, S. Sponar, and Y. Hasegawa, Fundamental phenomena of quantum mechanics explored with neutron interferometers, Prog. Theor. Exp. Phys **2014**, (2014).

[28] S. Sponar, R. I. P. Sedmik, M. Pitschmann, H. Abele, and Y. Hasegawa, Tests of fundamental quantum mechanics and dark interactions with low-energy neutrons, Nat. Rev. Phys **3**, 309 (2021).

[29] T. Denkmayr, H. Geppert, H. Lemmel, M. Waegell, J. Dressel, Y. Hasegawa, and S. Sponar, Experimental demonstration of direct path state characterization by strongly measuring weak values in a matter-wave interferometer, Phys. Rev. Lett. **118**, 010402 (2017).

[30] R. Wagner, W. Kersten, A. Danner, H. Lemmel, A. K. Pan, and S. Sponar, Direct experimental test of commutation relation via imaginary weak value, Phys. Rev. Research **3**, 023243 (2021).

[31] H. Geppert-Kleinrath, T. Denkmayr, S. Sponar, H. Lemmel, T. Jenke, and Y. Hasegawa, Multifold paths of neutrons in the three-beam interferometer detected by a tiny energy kick, Phys. Rev. A **97**, 052111 (2018).

[32] H. Lemmel, N. Geerits, A. Danner, H. F. Hofmann, and S. Sponar, Quantifying the presence of a neutron in the paths of an interferometer, Phys. Rev. Research **4**, 023075 (2022).

[33] S. Sponar, E. Kreuzgruber, and H. Lemmel, "Leggett-Garg Inequality," (2019), https://doi.ill.fr/10.5291/ILL-DATA.CRG-2643.

[34] D. Petrascheck and H. Rauch, Multiple Laue rocking curves, Acta Crystallogr. A **40**, 445 (1984).